RadioGraphics

Best Cases from the AFIP

Glioblastoma Multiforme[1]

David A. Altman, MD • Denis S. Atkinson, Jr, MD • Daniel J. Brat, MD, PhD

Editor's Note.—Everyone who has taken the course in radiologic pathology at the Armed Forces Institute of Pathology (AFIP) remembers bringing beautifully illustrated cases for accession to the Institute. In recent years, the staff of the Department of Radiologic Pathology has judged the "best cases" by organ system, and recognition is given to the winners on the last day of the class. With each issue of *RadioGraphics*, one or more of these cases are published, written by the winning resident. Radiologic-pathologic correlation is emphasized, and the causes of the imaging signs of various diseases are illustrated.

History

An 80-year-old man with a remote history of prostate cancer fell and struck the left side of his head. He did not recall the details of the fall and had to be awakened afterward. The patient exhibited persistent difficulty with balance and memory, and he was taken to the emergency department, where computed tomography (CT) of the head yielded abnormal findings. Results of magnetic resonance (MR) imaging of the brain confirmed the presence of a heterogeneously enhancing lesion in the posterior left temporal lobe. CT of the chest, abdomen, and pelvis was negative for metastatic disease. On being questioned, the patient reported occasional bilateral temporal headaches; right-sided weakness; and escalating impairment of hearing, speech, concentration, and memory.

Upon admission, the patient was started on decadron, resulting in significant improvement in speech impairment and weakness. On the fifth day after admission, he underwent a single radiation treatment. In the early morning of the 11th day after admission, he was found dead. Autopsy was performed.

Abbreviations: NAA = N-acetylaspartate, WHO = World Health Organization

RadioGraphics 2007; 27:883–888 • **Published online** 10.1148/rg.273065138 • **Content Codes:** NR OI

[1]From the Departments of Radiology (D.A.A., D.S.A.) and Pathology (D.J.B.), Emory University School of Medicine, 1364 Clifton Rd NE, Atlanta, GA 30322. Received July 19, 2006; revision requested August 17 and received September 20; accepted September 22. All authors have no financial relationships to disclose. **Address correspondence to** D.A.A. (e-mail: *david.altman@aya.yale.edu*).

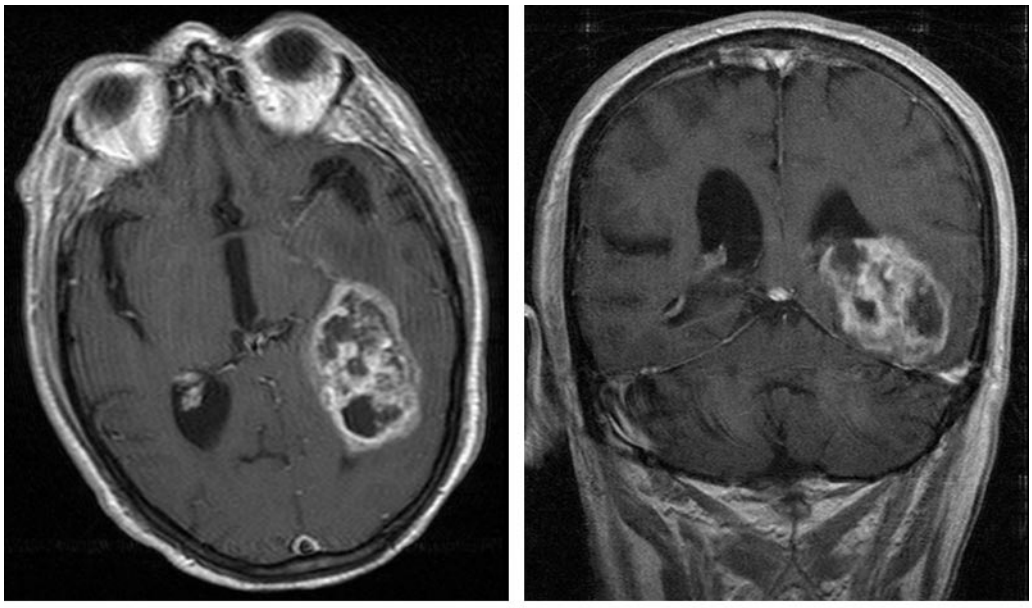

a. b.

Figure 1. Axial **(a)** and coronal **(b)** gadolinium-enhanced T1-weighted MR images demonstrate a heterogeneously enhancing mass with central necrosis centered in the posterior left temporal lobe.

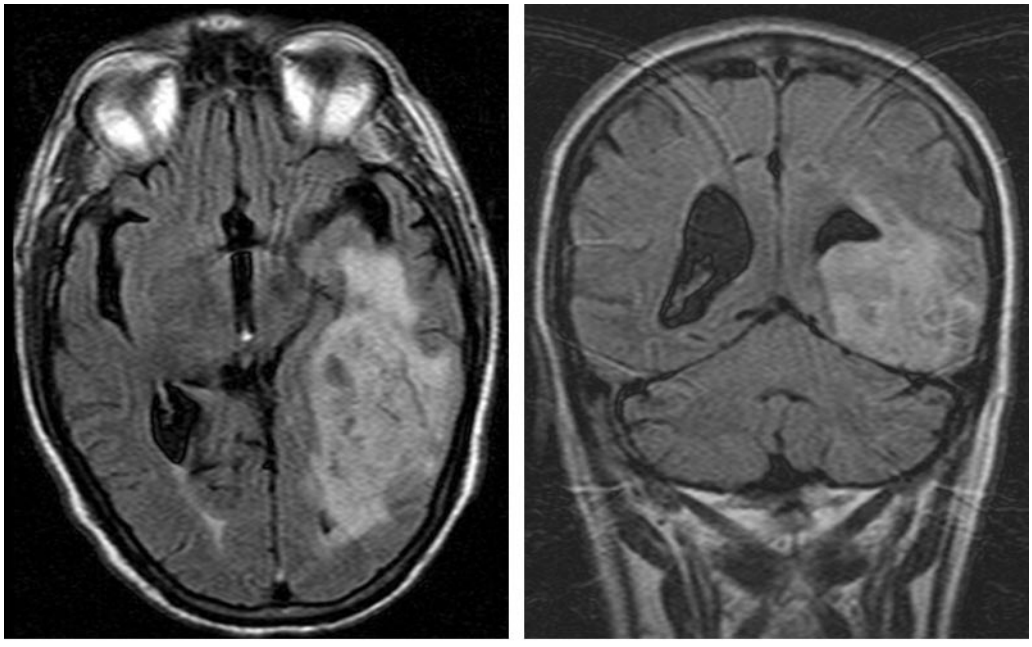

a. b.

Figure 2. Axial **(a)** and coronal **(b)** fluid-attenuated inversion recovery MR images demonstrate the mass with a large amount of surrounding T2 prolongation, a finding that suggests edema.

Imaging Findings

Gadolinium-enhanced MR imaging and MR spectroscopy of the brain were performed. MR images of the brain revealed a heterogeneously enhancing mass with central necrosis centered in the posterior left temporal lobe with involvement of the left parietal lobe and posterior insula (Fig 1). The enhancing portion of the mass measured 6.0 × 4.0 × 4.5 cm. There was local mass effect on the adjacent left lateral ventricle and a large amount of associated edema (Fig 2).

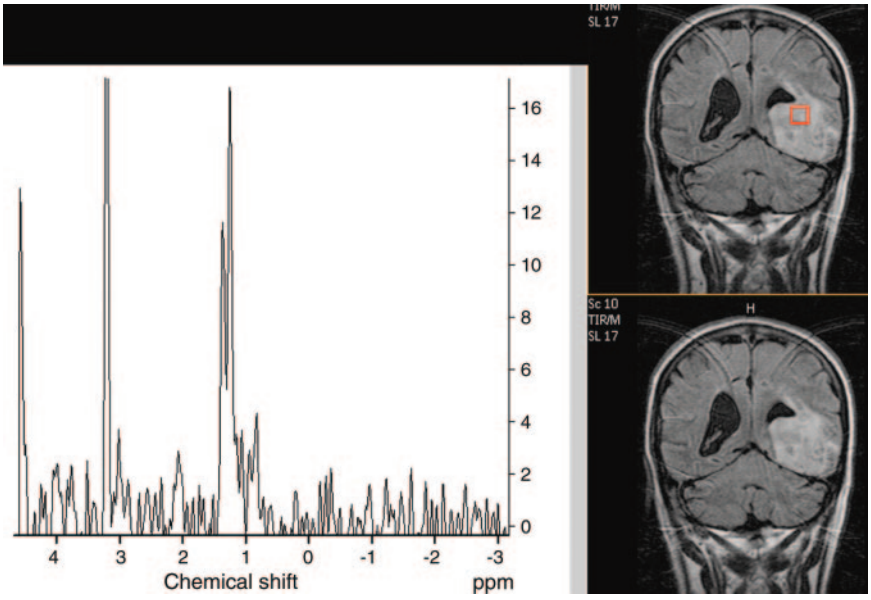

Figure 3. Image from single-voxel MR spectroscopy (echo time = 288 msec) demonstrates decreased levels of NAA and elevation of the choline-to-creatine ratio to more than 3:1, findings that suggest an aggressive neoplastic process. Red box indicates the site of interrogation.

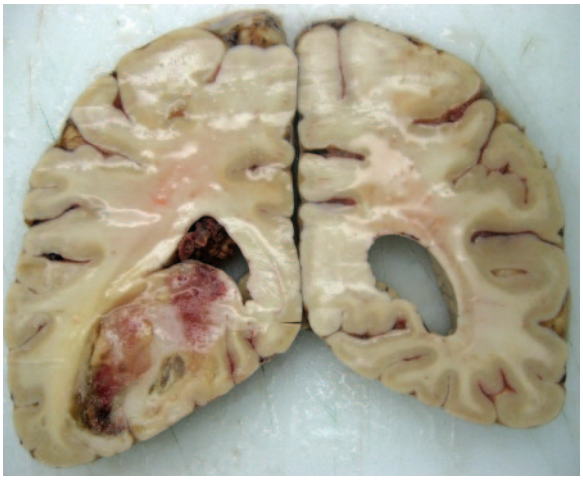

Figure 4. Photograph of the coronally sectioned gross pathologic brain specimen demonstrates an ill-defined, heterogeneous mass centered in the left temporal lobe. Areas of hemorrhage and necrosis are present, and the adjacent tissue is edematous.

Single-voxel MR spectroscopy with echo times of 144 and 288 msec was performed on the mass. Within the area of abnormality, the spectra exhibited decreased levels of N-acetylaspartate (NAA) and elevation of the choline-to-creatine ratio to more than 3:1, findings that suggest an aggressive neoplastic process (Fig 3). An elevated peak centered at 1.3 ppm was thought to represent lipid rather than lactate due to the absence of J coupling on 144-msec spectra. (At echo times near 144 msec, phase inversion of the signal occurs for lactate but not for lipid due to spin-spin interactions [1].)

Pathologic Evaluation

At postmortem examination, the surfaces of the brain showed no discrete lesions. The left temporoparietal region was enlarged and bulged outward but had a normal surface texture. No uncal or tonsillar herniation was noted at the base. Coronal sectioning revealed an ill-defined, 6-cm solitary mass centered in the left temporal lobe and extending into the left parietal lobe (Fig 4). The tumor was heterogeneous in color and texture, with multiple small areas that were softened, necrotic, hemorrhagic, and gelatinous alternating with regions that appeared more viable. The brain tissue adjacent to the mass was edematous, and the normal anatomic structures were displaced in all directions.

Multiple tissue sections of the tumor and adjacent brain were examined. The tumor was composed of malignant astrocytoma cells infiltrating the brain with a cell density that ranged from moderate to high and displayed all of the histopathologic features of a glioblastoma (World Health Organization [WHO] grade IV) (Fig 5). The central regions of the tumor were almost entirely necrotic, with only scattered islands of viable neoplastic tissue, mostly around blood vessels. Immediately adjacent to the central necrosis was densely cellular tumor tissue consisting of highly anaplastic astrocytoma cells with a fibrillar morphologic character. In addition to central coagulative necrosis, numerous smaller regions of

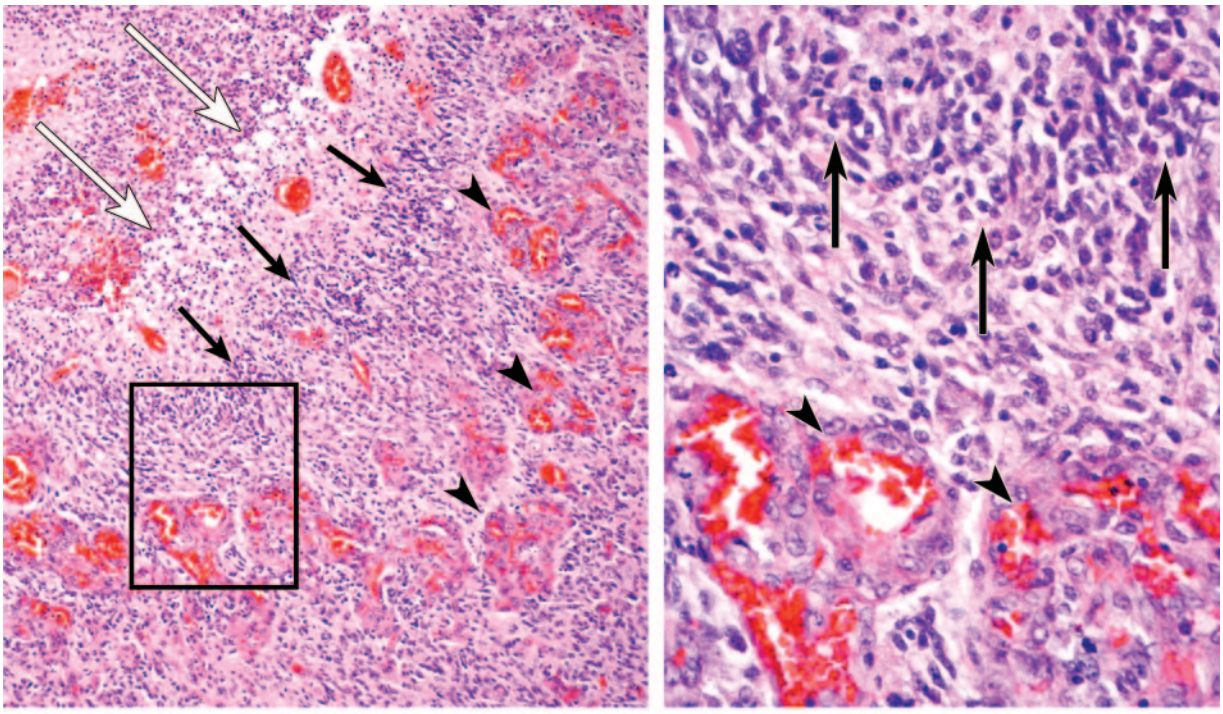

a. b.

Figure 5. Photomicrographs of the lesion (**b** [original magnification, ×600; hematoxylin-eosin stain] is a magnified view of the boxed area in **a** [original magnification, ×100; hematoxylin-eosin stain]) demonstrate regions of necrosis (white arrows) surrounded by rings of pseudopalisading tumor cells (black arrows), which are in turn surrounded by abundant microvascular hyperplasia (arrowheads).

necrosis surrounded by rings of pseudopalisading tumor cells were seen, a configuration known as pseudopalisading necrosis. Abundant microvascular hyperplasia was noted in the regions surrounding the pseudopalisading tumor cells. In many instances, hyperplastic vessels took the form of glomeruloid bodies, a highly proliferative budding of endothelial cells resembling a renal glomerulus. At the periphery of the tumor, extending widely into both the deep white matter and the overlying cortex, individual astrocytic tumor cells were noted diffusely infiltrating between neuronal and glial processes of the central nervous system neuropil.

Discussion

Glioblastoma multiforme (WHO grade IV astrocytoma) is the most common primary brain malignancy, accounting for 12%–15% of all intracranial neoplasms (2). The prognosis is uniformly grim. Despite undergoing standard treatments, which today include surgical resection, postoperative radiation therapy, and multiple protocols of chemotherapy, over 75% of patients die within 18 months. The prognosis has not changed significantly since the 1970s (2,3).

Glioblastoma occurs most frequently in the cerebral hemisphere of adults between 45 and 70 years of age. It is rare in the cerebellum and spinal cord, and fewer than 10% of cases are found in children, in whom the brainstem is affected more commonly than in adults (2).

Most glioblastomas arise without evidence of a lower-grade precursor lesion after a short clinical course of approximately 3 months. The mean age of patients who present with *primary glioblastoma* is 55 years. Glioblastomas may also arise from an existing astrocytoma that has undergone progression to a higher grade. These *secondary glioblastomas* are consequently characterized by a longer clinical course and are found in a younger patient population (mean age, 40 years) (4).

Conventional gadolinium-enhanced MR imaging is the standard technique for the evaluation of glioblastoma and typically demonstrates a large, heterogeneous mass in the cerebral hemisphere exhibiting necrosis, hemorrhage, and enhancement. In adults, the differential diagnosis for a solitary, heterogeneously enhancing intraaxial mass with necrosis also includes metastasis and abscess. Although metastatic disease exhibits a wide variety of appearances, the large size of the lesion and lack of multiplicity in this case suggest that a primary tumor is more likely. A brain abscess may also exhibit distinguishing imaging

findings. For example, an abscess will not typically exhibit an elevated choline-creatine ratio at MR spectroscopy.

Multiple advanced MR imaging techniques have been shown to improve both tumor detection and the prospective evaluation of tumor grade. In a study of grade II and grade III astrocytomas, peripheral disarrangement of fiber tracts at diffusion-tensor MR imaging was shown to correlate with higher grade (5). Both MR spectroscopy and perfusion MR imaging have been shown to be useful in prospective determination of tumor grade. At spectroscopy, elevation of choline and depression of NAA suggest tumor; metabolite ratios (choline-creatine, choline-NAA, NAA-creatine, myoinositol-creatine) exhibit relationships to tumor grade. At perfusion MR imaging, relative cerebral blood volume is increased in higher-grade astrocytomas (6,7). A recent study also suggests a direct relationship between the contrast transfer coefficient (K^{trans}, a reflection of both blood flow and endothelial permeability) and length of survival in high-grade gliomas (8). MR imaging is also widely used in the posttreatment evaluation of tumor. Combinations of abnormal enhancement patterns at conventional MR imaging, such as the presence of multiple lesions and corpus callosum involvement, have been shown to be more likely than individual findings to help distinguish necrosis from tumor progression (9). It is the rule at initial diagnosis that glioblastoma exhibits necrosis at both radiologic and pathologic examination. Indeed, necrosis is one of the imaging findings that helps distinguish glioblastoma multiforme from a lower-grade astrocytoma.

Why do tumors become necrotic? We are taught that large tumors outgrow their blood supply due to unrestricted proliferation, and that in spite of increased angiogenesis, there is central vascular insufficiency. This model may not be accurate in glioblastoma. Recent pathology literature suggests that the characteristic pathologic features of glioblastoma—necrosis with surrounding pseudopalisades and microvascular hyperplasia—may reflect an intrinsic prothrombotic or vaso-occlusive event within the tumor rather than insufficient blood supply. Effects of both vascular endothelial growth factor and increased neoplastic production of tissue factor may cause an intrinsic prothrombotic state (10–13).

Rather than being a consequence of rapid growth, the distinctive neuroimaging features of glioblastoma—emergence of enhancement and rapid peripheral expansion of the mass—may be secondary to an intrinsic vascular event mediated by factors overexpressed by the glioblastoma itself. A cascade of events is triggered by inherent prothrombotic–vaso-occlusive mechanisms: Microvascular occlusion is followed by local hypoxia and consequent outward migration of tumor cells in a peripheral wave. The characteristic waves of pseudopalisading cells are thought to represent actively migrating hypoxic tumor cells. Pathologic analysis supports this hypothesis: The wave of pseudopalisading cells is *less proliferative* than the adjacent astrocytoma cells. These pseudopalisading cells are not rapidly dividing cells that have "outgrown their blood supply" (10); they are oxygen-starved cells desperately seeking sustenance. This pathologic model provides a better explanation for the findings at radiologic and gross pathologic examination: swift peripheral expansion of an enhancing tumor with extensive central necrosis, unfailingly leading to a poor prognosis.

Nevertheless, progress is being made in the diagnosis and treatment of glioblastoma, and much of the work involves an understanding of the mutations and differential expression of genes that have been associated with both primary and secondary glioblastomas. Primary glioblastomas are associated with amplification and overexpression of the cell surface receptor EGFR, mutations in PTEN, and abnormalities in chromosome 10, among other factors. Secondary glioblastomas often exhibit mutations in TP53, as well as abnormalities in chromosomes 19q and 10q (4,14,15). These variations are increasingly being exploited as molecular targets for diagnosis and therapy (16). Many kinds of biomarkers are being investigated. A study in an animal model demonstrated that MR imaging could help detect the incorporation of magnetically labeled stem cells into the neovascularization accompanying glioma. Not only can such techniques be used directly to identify disease, but they also can facilitate therapy as potential vectors of treatment (17).

Systemic delivery of chemotherapeutic agents to a glioblastoma has only limited efficiency, and side effects can be severe. One alternative is delivery of therapy directly to the tumor bed. Small wafers containing chemotherapeutic agents can be implanted into the surgical bed during resection. More recently, directed therapies using multiple specific molecular targets have been developed. One such area of current research is the use of antibodies directed against the overexpressed

EGFR found in some glioblastomas (16). The goal of such research is not merely to generate more drugs for the treatment of glioblastoma; it is also to generate tools to assault specific types of glioblastomas. Ideally, an individualized genetic profile could be determined for each patient's tumor and a corresponding treatment plan designed.

References

1. Chang KH, Song IC, Kim SH, et al. In vivo single-voxel proton MR spectroscopy in intracranial cystic masses. AJNR Am J Neuroradiol 1998;19(3):401–405.
2. Kleihues P, Burger PC, Collins VP, Newcomb EW, Ohgaki H, Cavenee WK. Glioblastoma. In: Kleihues P, Cavenee WK, eds. Pathology and genetics of tumors of the nervous system. Lyon, France: IARC, 2000; 29–39.
3. Stark AM, Nabavi A, Mehdorn HM, Blömer U. Glioblastoma multiforme: report of 267 cases treated at a single institution. Surg Neurol 2005; 63:162–169.
4. Kleihues P, Louis DN, Scheithauer BW, et al. The WHO classification of tumors of the nervous system. J Neuropathol Exp Neurol 2002;61(3):215–225.
5. Goebell E, Paustenbach S, Vaeterlein O, et al. Low-grade and anaplastic gliomas: differences in architecture evaluated with diffusion-tensor MR imaging. Radiology 2006;239(1):217–222.
6. Law M, Yang S, Wang H, et al. Glioma grading: sensitivity, specificity, and predictive values of perfusion MR imaging and proton MR spectroscopic imaging compared with conventional MR imaging. AJNR Am J Neuroradiol 2003;24:1989–1998.
7. Stadlbauer A, Gruber S, Nimsky C, et al. Preoperative grading of gliomas by using metabolite quantification with high-spatial-resolution proton MR spectroscopic imaging. Radiology 2006; 238(3):958–969.
8. Mills SJ, Patankar TA, Haroon HA, Balériaux D, Swindell R, Jackson A. Do cerebral blood volume and contrast transfer coefficient predict prognosis in human glioma? AJNR Am J Neuroradiol 2006; 27:853–858.
9. Mullins ME, Barest GD, Schaefer PW, Hochberg FH, Gonzalez RG, Lev MH. Radiation necrosis versus glioma recurrence: conventional MR imaging clues to diagnosis. AJNR Am J Neuroradiol 2005;26:1967–1972.
10. Brat DJ, Van Meir EG. Vaso-occlusive and prothrombotic mechanisms of tumor hypoxia, necrosis, and accelerated growth in glioblastoma. Lab Invest 2004;84:397–405.
11. Hunter SB, Brat DJ, Olson JJ, von Deimling A, Zhou W, Van Meir EG. Alterations in molecular pathways of diffusely infiltrating glial neoplasms: application to tumor classification and anti-tumor therapy. Int J Oncol 2003;23:857–869.
12. Burger PC, Nelson JS, Boyko OB. Diagnostic synergy in radiology and surgical neuropathology: neuroimaging techniques and general interpretive guidelines. Arch Pathol Lab Med 1998;122(7): 609–619.
13. Rong Y, Durden DL, Van Meir EG, Brat DJ. "Pseudopalisading" necrosis in glioblastoma: a familiar morphologic feature that links vascular pathology, hypoxia, and angiogenesis. J Neuropathol Exp Neurol 2006;65(6):529–539.
14. Wang SI, Puc J, Li J, et al. Somatic mutations of PTEN in glioblastoma multiforme. Cancer Res 1997;57:4183–4186.
15. Rasheed BK, Stenzel TT, McLendon RE, et al. PTEN gene mutations are seen in high-grade but not in low-grade gliomas. Cancer Res 1997;57: 4187–4190.
16. Phuphanich S, Brat DJ, Olson JJ. Delivery systems and molecular targets of mechanism-based therapies for GBM. Expert Rev Neurother 2004;4(4): 649–663.
17. Anderson SA, Glod J, Arbab AS, et al. Noninvasive MR imaging of magnetically labeled stem cells to directly identify neovasculature in a glioma model. Blood 2005;105:420–425.